Chapter 3
Urine Concentration

Abstract During water deprivation, the kidney of a mammal can conserve water by producing a urine that is more concentrated than blood plasma. That hypertonic urine is produced when water is reabsorbed, in excess of solutes, from the collecting ducts and into the renal vasculature, thereby concentrating the collecting duct fluid, which eventually emerges as urine. In this chapter, we introduce mathematical models that simulate the urine concentrating process. To learn how to build those models, we first derive equations that represent tubular flow, transmural water flux, and transmural solute fluxes along a renal tubule. We then develop models that simulate countercurrent multiplication in a loop, and we study factors that affect the efficiency of the concentrating mechanism.

3.1 Biological Background: How Does an Animal Produce a Concentrated Urine?

When a mammal is deprived of water, its kidney can conserve water by increasing solute concentration (or, osmolality) in urine to a level well above that of blood, so that solutes are excreted in excess of water. This process of urine concentration occurs in the renal medulla, and has the effect of stabilizing blood plasma osmolality. Some animals can concentrate urine better than others. Maximum reported urine osmolalities in several animals are shown in Table 3.1. For comparison, blood plasma osmolality is $\sim$300 mOsm/kg H_2O. The values in Table 3.1 indicate that the human kidney can produce a urine that is $\sim$4.8 times more concentrated than that of plasma. Note that is the *maximum* value ever measured, so it is fair to say that most of us don't do that well. That human maximum urine osmolality value is also the reason that one should refrain from drinking sea water to quench thirst, given that sea water osmolality ranges from 2,000 to 2,400 mOsm/kg H_2O. The kidney of an Australian hopping mouse, which lives in the desert, can produce an amazingly concentrated urine that has an osmolality $>$30 times above that of blood plasma.

A.T. Layton and A. Edwards, *Mathematical Modeling in Renal Physiology*, Lecture Notes on Mathematical Modelling in the Life Sciences, DOI 10.1007/978-3-642-27367-4_3,

Table 3.1 Maximum measured urine osmolalities in selected animals. For comparison, blood plasma osmolality is about 300 mOsm/kg H_2O

Animal	Urine osmolality mOsm/kg H_2O
Domestic pig	1,075
Human	1,430
Rat	2,849
Mouse	2,950
Chinchilla	7,599
Australian hopping mouse	9,374

A urine that has an osmolality higher than blood plasma is said to be hypertonic. A hypertonic urine is concentrated in the final stages of urine production: water is absorbed, in excess of solutes, from the collecting ducts and into the vasculature of the medulla, thus increasing the osmolality of the collecting duct fluid—fluid that is called urine after it emerges from the collecting ducts. In the outer medulla, water absorption from the collecting ducts is driven by the active transepithelial transport of NaCl from the water-impermeable thick ascending limbs into the surrounding interstitium, where the NaCl promotes, via osmosis, water absorption from collecting ducts, descending limbs, and some blood vessels. The countercurrent configuration of renal tubules and blood vessels in the outer medulla augments this concentrating effect, as a function of depth, along the cortico-medullary axis, so that an osmolality gradient is generated along all the structures of the outer medulla, from the cortico-medullary boundary to the outer-inner medullary boundary. Although this concentrating mechanism is well-established in the outer medulla—by both physiological experiments and theoretical investigation—the nature of the concentrating mechanism in the inner medulla remains to be elucidated.

3.2 Modeling Flow Along a Renal Tubule

In this section, we will derive equations that model tubular flow and transmural fluxes along a renal tubule. The system is assumed to be at steady state.

3.2.1 Mass Conservation Equations

We will derive the differential equations that describe the conservation of water and solutes along a renal tubule. We will first consider water transport along the tubule, which extends from $x = 0$ to $x = L$, as shown in Fig. 3.1. For simplicity, we assume that the tubule is rigid. Of course, technically speaking, tubular walls are comprised of cells that are, to some extent, flexible. However, the structures surrounding the tubules in vivo likely reduce that degree of compliance, which makes the rigid-wall

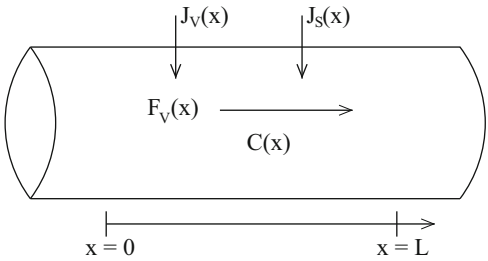

Fig. 3.1 Schematic drawing for model renal tubule, illustrating water flow (F_V), water flux (J_V), and solute flux (J_S)

assumption reasonable. It is also reasonable to describe the flow in the tubules as plug flow (i.e., flow with no radial component and constant velocity across any cross-section).

To derive a differential equation that describes water conservation along the tubule, consider the tubular segment in Fig. 3.1. The change in water flow rate must equal the sum of the water flux out of (or into) the tubule through its walls between $x = 0$ and $x = L$. This reasoning can be written as

$$F_V(L) = F_V(0) + 2\pi r \int_0^L J_V(x)\, dx, \tag{3.1}$$

where r denotes tubular radius, assumed constant. $F_V(x)$ denotes the volume flow rate along the tubule, the units of which are typically nl/min for renal tubules. $J_V(x)$ denotes water flux through the tubular walls, taken positive into the tubule. J_V is computed at a point along the circumference of the tubule, hence the multiplication by the factor $2\pi r$. Rewriting Eq. (3.1) in differential form, we get

$$\frac{\partial}{\partial x} F_V(x) = 2\pi r J_V(x). \tag{3.2}$$

Next we consider solute conservation along the tubule. Such a solute can be NaCl or urea or protein. The rate of flow of a given solute at position x is given by the product of its concentration $C(x)$ and the rate of flow of water $F_V(x)$, i.e., $F_V(x)C(x)$. Let the amount of solute transported inward through the tubule walls at x per unit area per unit time be denoted by $J_S(x)$. Then, through a procedure similar to the one we used to derive the water conservation equation (3.2), we can describe the solute conservation along the renal tubule by

$$\frac{\partial}{\partial x} \left(F_V(x)C(x)\right) = 2\pi r J_S(x). \tag{3.3}$$

The conservation equations (3.2) and (3.3) are general and apply to all types of renal tubules. Of course, tubules in the kidney differ widely in their transport properties, and those differences are reflected in the flux terms J_V and J_S.

3.2.2 Water Fluxes

Water can be driven through a cell membrane by hydrostatic pressure, oncotic pressure, and osmotic pressure. Oncotic pressure, discussed in Chap. 4, is exerted by proteins in blood plasma. Because in a healthy kidney, virtually no proteins are filtered by the glomerulus, oncotic pressure can be assumed to be zero along the loops of Henle and collecting ducts.

Osmotic pressure is the pressure that must be applied to a solution to stop the inflow of water across a water-permeable membrane. Water tends to move through a water-permeable membrane when the solutions on the two sides of the membrane have different *osmolalities*. Osmolality is given by a weighted sum of the concentrations of all the solutes in the solution:

$$\text{osmolality} = \sum_k \sigma_k C_k, \tag{3.4}$$

where C_k is the concentration of the kth solute, and σ_k is the osmotic coefficient of that solute.

Consider a membrane that is permeable to water but impermeable to a given solute. Suppose the difference in the concentration of that solute between the two sides of the membrane is ΔC. Then, for a small solute, the osmotic pressure exerted by that solute can be approximated by

$$\text{osmotic pressure} = RT\sigma\Delta C, \tag{3.5}$$

where R is the universal gas constant ($62.36 \times 10^{-3}\text{mmHg}\cdot K^{-1}\cdot\text{mM}^{-1}$), and T is the absolute temperature. Even a small concentration gradient can exert a substantial osmotic pressure. Let $\Delta C = 1\,\text{mM}$, $\sigma = 1$, and $T = 310.15\,\text{K}$ (human body temperature, $\approx$37 C). The osmotic pressure is about 19.3 mmHg.

Hydrostatic pressure is frequently assumed negligible, because the transmembrane hydrostatic pressure difference, which is likely on the order of 1 mmHg, is much smaller than the osmotic pressure exerted by a concentration gradient of 1 mM (which is $\sim$19.3 mmHg).

To derive the equation that describes water flux across a renal tubule, we make another simplifying assumption, which is that water transport across tubular walls can be represented as single-barrier transport. We make the same assumption in our description of solute fluxes below as well. Renal tubular and vascular walls are made up of a single layer of cells (epithelial cells for loops of Henle and collecting ducts, and endothelial cells for vasa recta). A fluid or solute particle can be transported through the cells, or paracellularly through the junctions between cells. To move from the tubular lumen through the cells into the surrounding interstitium, the particle must first move through the apical cell membrane into the cytoplasm of the cell, diffuse through the cytoplasm, and then move through

a second cell membrane, the basolateral membrane. The transport properties of the two cell membranes (apical and basolateral) are often different. However, because the transport properties of individual membranes are frequently not well known, and because transcellular transport can be complicated, we assume that the transport between luminal and interstitial compartments can be represented as a single-barrier flux.

Given the above discussion, water flux into a renal tubule in Fig. 3.1 can be described by

$$J_V(x) = L_p(x)RT\sigma\left(C(x) - C^e(x)\right), \tag{3.6}$$

where $L_p(x)$ is the water permeability of the tubule, and $C^e(x)$ denotes the interstitial (i.e., external) solute concentration at position x. As discussed above, oncotic and hydrostatic pressures are assumed negligible. For this simple model, only one solute is represented. If multiple solutes are represented, the osmotic pressure is given by a summation as in Eq. (3.4).

3.2.3 *Solute Fluxes*

Transepithelial solute fluxes may be driven by electrochemical potential gradients, by pumps (i.e., active transport), or via coupled transport systems. In Chap. 8 we discuss how to model these fluxes in details. Here we take a simpler approach and make the same single-barrier transport assumption that we have made for water fluxes. A typical simple model considers two pathways by which a solute may be transported across renal tubular walls, passive and active:

$$J_S(x) = -\frac{V_{\max}(x)C(x)}{K_M + C(x)} + P_S(x)\left(C^e(x) - C(x)\right). \tag{3.7}$$

For simplicity, the solute is assumed to be uncharged (e.g., urea or NaCl). The first term on the right represents active solute transport, characterized by Michaelis-Menten kinetics, which is one of the simplest and best-known models of enzyme kinetics in biochemistry, named after German biochemist Leonor Michaelis and Canadian physicist Maud Menten. Here, $V_{\max}$ represents the maximum transport rate achieved by the system at solute concentration C, and the Michaelis constant K_M is the solute concentration at which the reaction rate is half of $V_{\max}$. Thus, the transport rate increases as C increases from 0, but it levels off and approaches $V_{\max}$ as C approaches infinity. The negative sign implies that the active transport flux is outward-directed. The second term in the equation represents transmural diffusion, with solute permeability P_S.

3.3 Countercurrent Multiplication in a Loop

We will develop a model of the loop of Henle that illustrates the principle of countercurrent multiplication. The paradigm of countercurrent multiplication was proposed by Werner Kuhn, a brilliant Swiss physical chemist who had studied with giants such as Niels Bohr and Ernest Rutherford. With his colleague Kaspar Ryffel, Kuhn published a 34-page treatise describing and actually testing several arrangements by which an osmolality gradient could be generated along parallel but opposing flows in adjacent tubes that were made contiguous by a hair-pin turn. By the principle of *countercurrent multiplication*, a transfer of solute from one tubule to another (a "single" effect) augments ("multiplies," or reinforces) the axial osmolality gradient in the parallel flow ("Vervielfältigung des Einzeleffektes"). Thus, a small transverse osmolality difference (a small single effect) is multiplied into a much larger osmolality difference along the axis of tubular flow.

To exemplify the principle of countercurrent multiplication, we will construct a model that represents a loop, with a descending limb and an ascending limb. The two limbs are assumed to be in direct contact with each other. A schematic diagram of the model configuration is shown in Fig. 3.2a. The model represents only one solute, say, NaCl. In addition, we make the following simplifying assumptions:

1. We assume that the descending limb is water impermeable but infinitely permeable to solute. This is of course a simplification, because a large portion of the descending limb is known to be highly water permeable. Nonetheless, we make this assumption to make things easy. The conservation equations become

$$\frac{\partial}{\partial x} F_{\mathrm{DL},V}(x) = 0, \tag{3.8}$$

$$\frac{\partial}{\partial x} \left(F_{\mathrm{DL},V}(x) C_{\mathrm{DL}}(x)\right) = 2\pi r_{\mathrm{DL}} J_{\mathrm{DL},S}(x), \tag{3.9}$$

   where the subscript 'DL' denotes the descending limb.
2. We assume that the ascending limb is water impermeable. And we assume that the solute is pumped out of the ascending limb at a fixed rate of A. A fixed pump rate is assumed instead of the (nonlinear) Michaelis-Menten kinetics in Eq. (3.7) so that we can derive an analytical solution. Additionally, we assume that all of that solute goes into the descending limb. Thus, $2\pi r_{\mathrm{DL}} J_{\mathrm{DL},S} = A$ and $2\pi r_{\mathrm{AL}} J_{\mathrm{AL},S} = -A$, where the subscript 'AL' denotes the ascending limb. The conservation equations for the ascending limb are

$$\frac{\partial}{\partial x} F_{\mathrm{AL},V}(x) = 0, \tag{3.10}$$

$$\frac{\partial}{\partial x} \left(F_{\mathrm{AL},V}(x) C_{\mathrm{AL}}(x)\right) = -A. \tag{3.11}$$

3. Because the descending and ascending limbs are assumed to be contiguous, at the loop bend ($x = L$) we have

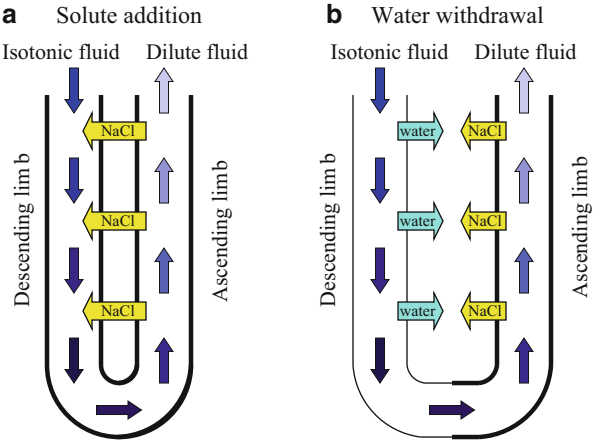

Fig. 3.2 Two paradigms for countercurrent multiplication. (**a**) Countercurrent multiplication by NaCl transfer from an ascending flow to a descending flow: the concentration of the descending flow is progressively concentrated by NaCl addition. (**b**) Countercurrent multiplication by water withdrawal from a descending flow: NaCl transport from the ascending flow into the interstitium raises interstitial osmolality; this results in passive water transport from the descending flow, which has lower osmolality than the interstitium. In both paradigms, a steady state is achieved in which NaCl concentration is raised in the descending limb so that tubular fluid achieves a maximum concentration at the loop bend. In both figure panels, tubular fluid flow direction is indicated by *blue arrows*; increasing osmolality is indicated by *darkening shades of blue*. *Thick black lines* indicate that a tubule is water impermeable; *thin lines* indicate high permeability to water (Figure modified from Layton and Layton 2011)

$$F_{\mathrm{DL},V}(L) = -F_{\mathrm{AL},V}(L), \tag{3.12}$$

$$C_{\mathrm{DL}}(L) = C_{\mathrm{AL}}(L). \tag{3.13}$$

In Eq. (3.12) we assume that flow is positive in the x direction; thus, flow rate along the ascending limb is negative.

4. Finally, to complete the system, we must specify the boundary conditions at the entrance of the descending limb:

$$F_{\mathrm{DL},V}(0) = F_{V,0}, \tag{3.14}$$

$$C_{\mathrm{DL}}(0) = C_0. \tag{3.15}$$

We now have enough information to determine $C_{\mathrm{DL}}(x)$ and $C_{\mathrm{AL}}(x)$. Since the entire loop is assumed to be water impermeable, $F_{\mathrm{DL},V}(x) = F_{V,0}$ and $F_{\mathrm{AL},V}(x) = -F_{V,0}$. Plugging this into Eq. (3.9), we have

$$F_{V,0}\frac{\partial}{\partial x}C_{\mathrm{DL}}(x) = A, \tag{3.16}$$

which can be integrated, and combined with the boundary condition (3.15), to yield

$$C_{\mathrm{DL}}(x) = C_0 + \left(\frac{A}{F_{V,0}}\right) x. \tag{3.17}$$

Now to compute solute concentration along the ascending limb, we evaluate C_{DL} at $x = L$, use that as the initial condition for the ODE (3.11) to get

$$\begin{aligned} C_{\mathrm{AL}}(x) &= C_{\mathrm{DL}}(L) - \left(\frac{A}{F_{V,0}}\right)(L - x) \\ &= C_0 + \left(\frac{A}{F_{V,0}}\right) x = C_{\mathrm{DL}}(x). \end{aligned} \tag{3.18}$$

This simple model predicts that (1) the concentrations along the descending and ascending limbs are the same at any given position x; (2) solute concentration increases linearly along the x direction; and thus (3) the longer the loop, the higher the loop-bend concentration.

3.4 Countercurrent Multiplication in a Loop, Revisited

The preceding example assumes that solute is directly secreted from the ascending limb into the descending limb. While experimental studies support active NaCl transport from thick ascending limbs, experiments also indicate that descending limbs are not highly permeable to NaCl. Instead, those segments of the descending limbs are highly permeable to water. These observations suggest that the accumulation of NaCl from thick limbs may concentrate descending limb tubular fluid principally by means of osmotic water absorption from descending limbs rather than by NaCl secretion into descending limbs. We will modify our model to capture this mechanism.

A schematic diagram of the model is shown in Fig. 3.2b. We assume that the descending and ascending limbs of the loop interact through a common, external compartment, which represents extratubular structures, such as the interstitium, interstitial cells and vasculature. Both the NaCl that is actively pumped out of the ascending limb and the water that is reabsorbed from the descending limb are taken up by the external compartment.

3.4.1 Model Assumptions

Here are the new model assumptions:

1. We assume that the descending limb is impermeable to solute, but is highly permeable to water. In fact, we assume the descending limb is so permeable

to water that its concentration equilibrates with the external solute concentration C^e, i.e.,

$$C_{\mathrm{DL}}(x) = C^e(x). \tag{3.19}$$

The solute conservation equation is

$$\frac{\partial}{\partial x}\left(F_{\mathrm{DL},V}(x)C_{\mathrm{DL}}(x)\right) = 0, \tag{3.20}$$

since there is no solute flux, i.e., $J_{\mathrm{DL},S}(x) = 0$. The water conservation equation is

$$\frac{\partial}{\partial x}F_{\mathrm{DL},V}(x) = 2\pi r_{\mathrm{DL}}J_{\mathrm{DL},V}(x). \tag{3.21}$$

2. The conservation equations for the ascending limb are the same as before: Eqs. (3.10) and (3.11).
3. For the external compartment, we assume that the reabsorbate (i.e., NaCl from the ascending limb and water from the descending limb) is picked up locally. That is, we assume no axial flow in this compartment. Thus, by mass conservation, the external compartment concentration $C^e(x)$ can be related to the solute and water fluxes by

$$C^e(x) = \frac{2\pi r_{\mathrm{AL}}J_{\mathrm{AL},S}(x)}{2\pi r_{\mathrm{DL}}J_{\mathrm{DL},V}(x)} = -\frac{A}{2\pi r_{\mathrm{DL}}J_{\mathrm{DL},V}(x)}. \tag{3.22}$$

3.4.2 Model Solution

We will first compute water flow and solute concentration along the descending limb. Equation (3.20) implies that, because the descending limb is solute-impermeable, solute flow is constant along the limb. That is, we can write

$$F_{\mathrm{DL},V}(x)C_{\mathrm{DL}}(x) = F_{\mathrm{DL},V}(0)C_{\mathrm{DL}}(0), \tag{3.23}$$

$$\Rightarrow F_{\mathrm{DL},V}(x) = F_{\mathrm{DL},V}(0)\frac{C^e(0)}{C^e(x)}. \tag{3.24}$$

since we assume that the descending limb concentration equilibrates with the external concentration. To get $C^e(x)$, we eliminate $J_{\mathrm{DL},V}(x)$ from Eq. (3.21) using Eq. (3.22) to get

$$\frac{\partial}{\partial x}F_{\mathrm{DL},V}(x) = -\frac{A}{C^e(x)}. \tag{3.25}$$

We then rewrite Eq. (3.20) as

$$C^e(x)\frac{\partial}{\partial x}F_{\mathrm{DL},V}(x) + F_{\mathrm{DL},V}(x)\frac{\partial}{\partial x}C^e(x) = 0, \tag{3.26}$$

with $C_{\mathrm{DL}}(x)$ replaced by $C^e(x)$. Next, we eliminate $F_{\mathrm{DL},V}$ and its spatial derivative from the above equation, using Eqs. (3.24) and (3.25):

$$A = F_{\mathrm{DL},V}(0)\frac{C^e(0)}{C^e(x)}\frac{\partial}{\partial x}C^e(x), \tag{3.27}$$

which can be written as

$$\frac{\partial}{\partial x}C^e(x) = \frac{A}{F_{\mathrm{DL},V}(0)C^e(0)}C^e(x). \tag{3.28}$$

The ODE can be integrated to give the solute concentrations along the external compartment as well as the descending limb:

$$C^e(x) = C_{\mathrm{DL}}(x) = C^e(0)\exp\left(\frac{Ax}{F_{\mathrm{DL},V}(0)C^e(0)}\right). \tag{3.29}$$

The above solution indicates that the descending limb and external solute concentrations increase exponentially along the model medulla.

Now let's consider the ascending limb. To compute its flow rate and concentration, we need its boundary conditions, i.e., flow rate and concentration at the loop bend. By evaluating Eqs. (3.24) and (3.29) at $x = L$, we have

$$F_{\mathrm{AL},V}(L) = -F_{\mathrm{DL},V}(L) = -F_{\mathrm{DL},V}(0)\frac{C_{\mathrm{DL}}(0)}{C^e(L)}, \tag{3.30}$$

$$C_{\mathrm{AL}}(L) = C^e(L) = C^e(0)\exp\left(\frac{AL}{F_{\mathrm{DL},V}(0)C^e(0)}\right). \tag{3.31}$$

Because the ascending limb is assumed to be water impermeable, its water flow rate doesn't change, i.e., $F_{\mathrm{AL},V}(x) = F_{\mathrm{AL},V}(L)$. Its solute concentration does change, though. In fact, we expect it to progressively decrease towards $x = 0$ as NaCl is actively pumped out. Using Eq. (3.31) as the initial condition for the solute conservation equation (3.11), we obtain

$$C_{\mathrm{AL}}(x) = C^e(0)\exp\left(\frac{AL}{F_{\mathrm{DL},V}(0)C^e(0)}\right) - \frac{Ax}{F_{V,DL}(L)}. \tag{3.32}$$

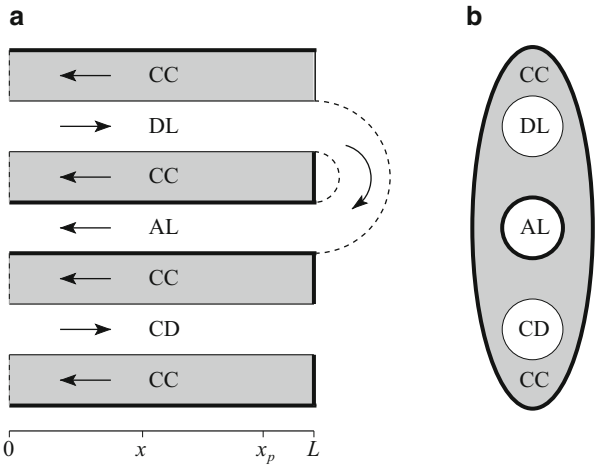

Fig. 3.3 Schematic diagram of the central core model. Panel (**a**), tubules along spatial axis. *DL* descending limb, *AL* ascending limb, *CD* collecting duct, *CC* central core. *Arrows*, steady-state flow directions. *Heavy lines*, water-impermeable boundaries. Panel (**b**), cross-section showing connectivity between CC and other tubules (Reprinted from Layton and Layton 2002)

3.5 The Central Core Model

In the model we have just considered, water and solute absorbed from tubules into the interstitium are assumed to enter the peritubular capillaries directly, at each medullary level, and afterwards, that absorbate is assumed to have no further interaction with the medulla, because we assume that there is no axial flow outside of the loop. Consequently, relatively concentrated ascending fluid does not equilibrate with progressively less concentrated surrounding interstitium. And as a result, that model may be unrealistically dissipative of the axial osmolality gradient.

We now consider an alternative model formulation, the *central core assumption*. A schematic diagram of the central core model is shown in Fig. 3.3. The central core was developed by John Stephenson (1955–2010), a former faculty member at the Weill Cornell Medical College in New York City. In the central core formulation, blood vessels, interstitial cells, and interstitial spaces are merged into a single compartment, with which the loops of Henle and collecting ducts interact. Axial flow is allowed within the central core. The central core formulation assumes maximum countercurrent exchange by the vasculature, and, compared to the model in Sect. 3.4, is much less dissipative of the axial osmolality gradient. The effects of the vasculature on the concentrating mechanism are considered in Chap. 4.

We augment the previous model (Sect. 3.4) in two ways. First, we use the central core assumption to represent the interactions among the tubules and the vasculature. Second, we also represent the collecting duct, which, together with the loops of Henle, are surrounded by, and interact through, a central core. The solute that is pumped out of the ascending limb, or the water and solute that are reabsorbed from

the descending limb and collecting duct, are picked up by the capillaries that are represented by the central core. Thus, by water and solute conservation, the water and solute fluxes into the central core are given by the sum of the corresponding tubular fluxes:

$$2\pi r_{\mathrm{CC}} J_{\mathrm{CC},V} = 2\pi \left(-r_{\mathrm{DL}} J_{\mathrm{DL},V} - r_{\mathrm{AL}} J_{\mathrm{AL},V} - r_{\mathrm{CD}} J_{\mathrm{CD},V}\right), \tag{3.33}$$

$$2\pi r_{\mathrm{CC}} J_{\mathrm{CC},S} = 2\pi \left(-r_{\mathrm{DL}} J_{\mathrm{DL},S} - r_{\mathrm{AL}} J_{\mathrm{AL},S} - r_{\mathrm{CD}} J_{\mathrm{CD},S}\right). \tag{3.34}$$

3.5.1 Model Assumptions

We make the following assumptions in this model:

1. We assume that the descending limb and collecting duct are infinitely water permeable. As a result, the intratubular concentrations of the descending limb and collecting duct nearly equilibrate with the central core, and, to a good approximation,

$$C_{\mathrm{DL}}(x) = C_{\mathrm{CD}}(x) = C_{\mathrm{CC}}(x) \equiv C(x). \tag{3.35}$$

   We denote the common concentration by $C(x)$.
2. The descending and ascending limbs are contiguous, and the boundary conditions Eqs. (3.12) and (3.13) hold.
3. We assume that the ascending limb is water impermeable. Thus, $J_{\mathrm{AL},V} = 0$, and it follows that $F_{\mathrm{AL},V}(x) = -F_{\mathrm{DL},V}(L)$ for all x.
4. We assume that the descending limb and collecting duct are solute permeable. Thus, from Eq. (3.34), we have

$$r_{\mathrm{DL}} J_{\mathrm{DL},S}(x) + r_{\mathrm{CD}} J_{\mathrm{CD},S}(x) + r_{\mathrm{CC}} J_{\mathrm{CC},S}(x) = -r_{\mathrm{AL}} J_{\mathrm{AL},S}(x). \tag{3.36}$$

5. We further assume that the central core is closed at $x = L$, which corresponds to the papillary tip. This assumption implies that there is no convective entry of solute or fluid at $x = L$. Thus, $F_{\mathrm{CC},V}(L) = 0$.

3.5.2 Model Solution

If we add up the solute conservation equations for the descending limb, collecting duct, and central core, we get

$$\frac{\partial}{\partial x}\left(F_{\mathrm{DL},V} C_{\mathrm{DL}} + F_{\mathrm{CD},V} C_{\mathrm{CD}} + F_{\mathrm{CC},V} C_{\mathrm{CC}}\right) = 2\pi \left(r_{\mathrm{DL}} J_{\mathrm{DL},S} + r_{\mathrm{CD}} J_{\mathrm{CD},S} + r_{\mathrm{CC}} J_{\mathrm{CC},S}\right), \tag{3.37}$$

or,

$$2\pi \left(r_{\mathrm{DL}} J_{\mathrm{DL},V} + r_{\mathrm{CD}} J_{\mathrm{CD},V} + r_{\mathrm{CC}} J_{\mathrm{CC},V}\right) C + \left(F_{\mathrm{DL},V} + F_{\mathrm{CD},V} + F_{\mathrm{CC},V}\right) \frac{\partial}{\partial x} C$$
$$= -2\pi r_{\mathrm{AL}} J_{\mathrm{AL},S}. \tag{3.38}$$

Because, by water conservation, $r_{\mathrm{DL}} J_{\mathrm{DL},S} + r_{\mathrm{CD}} J_{\mathrm{CD},S} + r_{\mathrm{CC}} J_{\mathrm{CC},S} = 0$, the above equation simplifies to an ODE for $C(x)$:

$$\frac{\partial}{\partial x} C(x) = \frac{-2\pi r_{\mathrm{AL}} J_{\mathrm{AL},S}}{F_{\mathrm{DL},V} + F_{\mathrm{CD},V} + F_{\mathrm{CC},V}}, \tag{3.39}$$

which says that the rate of increase of the concentration in the descending limb, collecting duct, and central core is the ratio of the solute reabsorption from the ascending limb to the net water flow rate in the other three tubules. Now we will rewrite the above equation in terms of the solute flow, given by $F_{i,S} = F_{i,V} C$ for tubule i. Dividing Eq. (3.39) by $C(x)$, we have

$$\frac{C'(x)}{C(x)} = \frac{-2\pi r_{\mathrm{AL}} J_{\mathrm{AL},S}}{F_{\mathrm{DL},S} + F_{\mathrm{CD},S} + F_{\mathrm{CC},S}}. \tag{3.40}$$

By solute conservation, we have for the collecting duct and central core

$$F_{\mathrm{CD},S}(x) = F_{\mathrm{CD},S}(0) + 2\pi r_{\mathrm{CD}} \int_0^x J_{\mathrm{CD},S}(s)\, ds, \tag{3.41}$$

$$F_{\mathrm{CC},S}(x) = -2\pi \int_L^x \left(r_{\mathrm{DL}} J_{\mathrm{DL},S}(s) + r_{\mathrm{CD}} J_{\mathrm{CD},S}(s) + r_{\mathrm{AL}} J_{\mathrm{AL},S}(s)\right) ds, \tag{3.42}$$

which together give

$$F_{\mathrm{CD},S}(x) + F_{\mathrm{CC},S}(x) = F_{\mathrm{CD},S}(L) - 2\pi \int_x^L \left(r_{\mathrm{DL}} J_{\mathrm{DL},S}(s) + r_{\mathrm{AL}} J_{\mathrm{AL},S}(s)\right) ds. \tag{3.43}$$

Upon substituting into Eq. (3.40), we get

$$\frac{C'(x)}{C(x)} = \frac{-2\pi r_{\mathrm{AL}} J_{\mathrm{AL},S}(x)}{F_{\mathrm{DL},S}(x) + F_{\mathrm{CD},S}(L) - 2\pi \int_x^L \left(r_{\mathrm{DL}} J_{\mathrm{DL},S}(s) + r_{\mathrm{AL}} J_{\mathrm{AL},S}(s)\right) ds}. \tag{3.44}$$

After integrating this ODE, we obtain the following expression

$$\frac{C(x)}{C(0)} = \exp\left(\int_0^x \frac{-2\pi r_{\mathrm{AL}} J_{\mathrm{AL},S}(y)}{F_{\mathrm{DL},S}(y) + F_{\mathrm{CD},S}(L) - 2\pi \int_y^L \left(r_{\mathrm{DL}} J_{\mathrm{DL},S}(s) + r_{\mathrm{AL}} J_{\mathrm{AL},S}(s)\right) ds}\, dy\right). \tag{3.45}$$

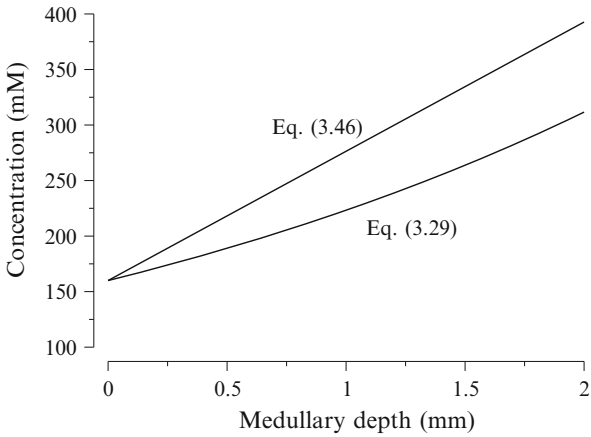

Fig. 3.4 A comparison of interstitial concentration profile $C(x)$ obtained using Eq. (3.29) for the countercurrent multiplication model in Sect. 3.4 with the profile obtained using Eq. (3.46) for the central core model in Sect. 3.5

The above expression, which is very general, gives the concentration ratio attained along the medulla as a function only of solute flow along the descending limb, flow exiting the end of the collecting duct, and the solute fluxes from the loop.

Now in the mammalian kidney, the descending limbs have a low permeability to NaCl. So let's assume $J_{DL,S} = 0$. As a result, $F_{DL,S}(x) = F_{DL,S}(0)$. We further assume that the solute is pumped out of the ascending limb at a fixed rate of A. With these assumptions, the integral (3.45) can be evaluated:

$$C(x) = C(0)\left(\frac{F_{DL,S}(0) + F_{CD,S}(L) - (L-x)A}{F_{DL,S}(0) + F_{CD,S}(L) - LA}\right). \tag{3.46}$$

Let's plug in some numbers and plot the above expression. Let's suppose $F_{DL,S}(0) = 1.6\,\text{nmol/min}$, $F_{CD,S}(L) = 0.2\,\text{nmol/min}$, $C(0) = 160\,\text{mM}$, and $L = 2\,\text{mm}$. We assume that 2/3 of the salt is pumped out of the ascending limb, consistent with what happens in the rat outer medulla; so $A = (2/3 \times 1.6)/2 = 0.533\,\text{nmol/(min·mm)}$. With these numbers, the fluid osmolality in the descending limb, collecting duct, and central core increases from 160 at $x = 0$ to 393 mOsm/kg H_2O at $x = L$, i.e., by a factor of 2.45.

What can we learn from the formula (3.46)? First, the higher the active transport rate of the ascending limb (A), the larger the concentrating effect. Second, the smaller the "load" on the concentrating mechanism, the larger the axial osmolality gradient. By "load" we mean the water flow rate of the descending limb and collecting duct. For example, if there is no urine "load" on the system, i.e., $F_{CD,S}(L) = 0$, then the descending limb and central core fluid will be concentrated to 480 mOsm/(kg H_2O), a factor of about 3.

To understand how the central core model solution compares with the earlier model in Sect. 3.4, which assumes that there is no axial flow outside of the loop, we calculate interstitial concentration profiles $C(x)$ for both models, using Eqs. (3.29) and (3.46). Those concentration profiles are shown in Fig. 3.4. As you can see,

the central core model produces a significantly higher concentrating effect. That is because axial flow within the central core allows absorbate from the deep medulla (i.e., closer to $x = L$), which has a high concentration, to interact with and concentrate the tubular fluid in the upper medulla (i.e., closer to $x = 0$), thereby augmenting the overall concentrating effect of the system.

3.6 The Distributed-Loop Model

Early models of the urine concentrating mechanism typically represent one loop of Henle and one collecting duct. These single-loop models may be sufficient to illustrate certain simple principles, e.g., countercurrent multiplication. But it has long been recognized that the loops of Henle differ from one another greatly. In the rat kidney, there are two populations of loops: the *short* loops of Henle, which turn near the boundary between the outer and inner medullas; and the *long* loops of Henle, which reach into the inner medulla. And not all long loops are alike either! Those long loops of Henle turn at differing depths of the inner medulla, some turn near the outer-inner medullary boundary, some reach deeper, and a small fraction reach all the way to the papillary tip.

Based on this observation, some models used the *discrete-loop representation*. Typically, such models represent a finite, usually small, number of loops. Say, two loops, one short loop and one long loop that reaches to the papillary tip. Some models represent a few more loops. But a rat kidney typically has approximately 30,000–40,000 loops, and it is simply not practical to represent each loop individually.

In his doctoral thesis, Harold Layton (now professor at Duke University) developed a model representation using *continuously distributed loops of Henle*. The reasoning is that because there are tens of thousands of loops of Henle in a kidney, we might as well assume a continuous distribution of those loops. We consider only one spatial direction that corresponds to the fluid flow direction, with the assumption that fluid flow and composition are homogeneous in the radial direction. However, we allow the tubular fluid flow rate and composition, as well as transmural fluxes, to differ among loops of different lengths. So each variable, e.g., solute concentration, is a function of two spatial variables x and y, i.e., $C(x, y)$. Here x denotes the location at which we are evaluating C, and y denotes the medullary depth at which the loop turns. With this notation, $C(x, y_1)$ and $C(x, y_2)$ denote the concentration values at location x of two different loops, one turning at depth y_1 and the other at y_2. $C(x_1, y)$ and $C(x_2, y)$ denote the concentration values of the same loop at two different locations, x_1 and x_2. We use the same notation for water flow $F_V(x, y)$, and fluxes $J_V(x, y)$ and $J_S(x, y)$ (Fig. 3.5).

A kidney likely behaves very differently if most of its loops are short and only a fraction are long (like in a rat), than if most of its loops are long ones (like in chinchilla). So we need a way to describe the population distribution of the loops. This can be done using a function $w(x)$ that specifies the fraction of loops that

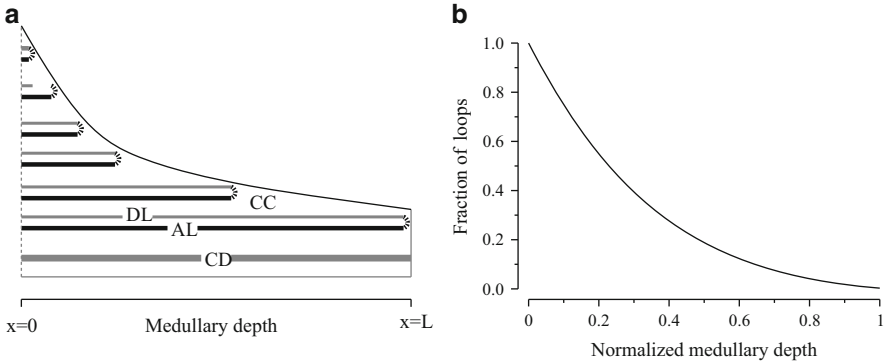

Fig. 3.5 Panel (**a**), schematic diagram of the distributed-loop model, showing loops of Henle (descending limb, *DL* and ascending limb, *AL*), collecting duct (*CD*), and central core (*CC*). Only six representative loops are drawn, but the model represents a continuously decreasing population. Panel (**b**), fraction of loops of Henle remaining ($w(x)$) as a function of medullary depth

remain at location x. So $w(x)$ is a monotonically decreasing function of x, starting at $w(0) = 1$ and decreasing to $w(L) = 0$ at the papillary tip.

As an example, we will revisit the central core model. This time, we replace the single loop in the previous example with a continuously distributed loop with population $w(x)$. Consider the sum of water fluxes into the central core at spatial location x. We must take into account water fluxes from the collecting duct, as well as from all loops that turn at a medullary level at or below x (i.e., at $x \leq y$). Loops with length shorter than x have already turned and thus make no contribution. The total water flux from all descending limbs that are present at x is given by

$$2\pi r_{\mathrm{DL}} \int_x^L J_{\mathrm{DL}}(x, y) \left(-\frac{dw(y)}{dy} \right) dy. \tag{3.47}$$

Since $w(y)$ is the fraction of loops remaining at level y, $-dw(y)/dy$ gives the rate at which loops turn at y. (Since w is monotonically decreasing, the negative sign gives us a positive rate.) Hence, Eq. (3.47) is the integral of water fluxes from all loops that turn beyond x, weighted by the population density of loops at each length. A similar integral is applied to the ascending limbs (but not the collecting duct). Together, the total water and solute fluxes into the central core are given by

$$\begin{aligned} 2\pi r_{\mathrm{CC}} J_{\mathrm{CC},V}(x) = &- 2\pi r_{\mathrm{DL}} \int_x^L J_{\mathrm{DL},V}(x, y) \left(-\frac{dw(y)}{dy} \right) dy \\ &- 2\pi r_{\mathrm{AL}} \int_x^L J_{\mathrm{AL},V}(x, y) \left(-\frac{dw(y)}{dy} \right) dy - 2\pi r_{\mathrm{CD}} J_{\mathrm{CD},V}(x), \end{aligned} \tag{3.48}$$

$$2\pi r_{CC} J_{CC,S}(x) = -2\pi r_{DL} \int_x^L J_{DL,S}(x,y) \left(-\frac{dw(y)}{dy}\right) dy - 2\pi r_{AL} \int_x^L J_{AL,S}(x,y) \left(-\frac{dw(y)}{dy}\right) dy - 2\pi r_{CD} J_{CD,S}(x). \tag{3.49}$$

Making the same assumptions as we did in Sect. 3.5 and following the derivation there, we obtain an expression for $C(x)$, which is the solute concentration for the central core, as well as the infinitely water-permeable descending limb and collecting duct:

$$\frac{C(x)}{C(0)} = \exp\left(\int_0^x \frac{2\pi r_{AL} \int_z^L -J_{AL,S}(z,y)(-w'(y))\, dy}{F^{tot}_{DL,S}(z) + F_{CD,S}(L) - J^{tot}_{loop,S}(z)}\, dz\right), \tag{3.50}$$

where $F^{tot}_{DL,S}(z) \equiv \int_z^L F_{DL,S}(z,y)(-w'(y))\, dy$ and

$$J^{tot}_{loop,S}(z) \equiv 2\pi \int_z^L \int_s^L r_{DL}(-w'(y)) J_{DL,S}(s,y) + r_{AL}(-w'(y)) J_{AL,S}(s,y)\, dy\, ds.$$

3.7 Current State of Affairs

The concentrating mechanism in the outer medulla of the mammalian kidney is believed to be well understood. That mechanism involves processes similar to those represented in the central core model in Sect. 3.5: the thick ascending limbs of the loop of Henle actively transport NaCl into the surrounding interstitium to generate an increasing osmolality gradient along all tubules and vessels.

However, the epithelial cells in the inner-medullary portion of the ascending limbs are very different from those in the outer medulla. In the inner medulla, those cells look "thinner" and have different transport properties. In particular, the thin ascending limbs found in the inner medulla have no significant active transepithelial transport of NaCl or of any other solute. As a result, active solute transport coupled with countercurrent flow does not explain the concentrating process in this region. This is particularly puzzling because the inner medulla is believed to be where the steepest osmotic gradient is generated.

Decades of efforts, both theoretical and experimental, have been dedicated to elucidating the urine concentrating mechanism of the inner medulla, which has remained one of the longest-standing mysteries in traditional physiology. Even though the inner medullary urine concentrating mechanism is still controversial, progress has been made. Anatomical studies have revealed that, perhaps unsurprisingly, the kidney is more complicated than we thought. New transporters continue to be discovered. As a result, our knowledge of the transport properties of the tubules,

as well as their interactions, is constantly revised. Mathematical models have been built to shed light into the roles of these new findings in the mammalian urine concentrating mechanism. For more details, you may refer to reviews by Layton (2002), Layton et al. (2009), and Pannabecker et al. (2008).

3.8 Problems

Problem 3.1. To a good approximation, the descending limbs of the loops of Henle in the Japanese quail kidney are water impermeable.

(a) Using the central core model described in Sect. 3.5, compute an expression for $R \equiv C(L)/C(0)$.

(b) Let

$$A = 2\pi \int_0^L (r_{\mathrm{DL}} J_{\mathrm{DL},S} + r_{\mathrm{AL}} J_{\mathrm{AL},S})\ dx. \tag{3.51}$$

Show that

$$\lim_{A \to F_{\mathrm{CD},S}(L)} R = \infty.$$

(c) Why is the relation $A > F_{\mathrm{CD},S}(L)$ prohibited in the model? Explain in terms of flows and concentrations.

(d) In the Japanese quail kidney, the descending limb is slightly water permeable, and, of course, there is a vasculature with counter-current exchange rather than a "central core." Also, $C_{\mathrm{CD}}(0) = C_{\mathrm{CC}}(0)$ will not be enforced. Explain why $A > F_{\mathrm{CD},S}(L)$ is a condition that will not be prohibited in a bird renal medulla. (Actual maximum avian concentration ratio R is about 2.)

Problem 3.2. In the outer medulla of the rat kidney, the lower half of about 2/3 of the descending limb is now thought to be water impermeable; the remaining descending limbs appear to be highly water permeable throughout the outer medulla. Assume that all descending limbs are solute impermeable.

(a) Assume that the collecting duct and the water-permeable population of the descending limbs are infinitely water permeable. Assume also that the ascending limbs are water impermeable, and have active solute transport that is independent of luminal solute concentration (but may depend on space). Using the central core framework, derive an expression for $R = C(L)/C(0)$.

(b) Let M be the total amount of solute entering all descending limbs. Assume that $J_{\mathrm{AL},S}$ is constant, that $2\pi r_{\mathrm{AL}} \int_0^L J_{\mathrm{AL},S}\ ds = M/2$, and that $F_{\mathrm{CD},S}(L) = M/10$. Evaluate R.

References

Layton, H.E.: Mathematical models of the mammalian urine concentrating mechanism. In: Layton, H.E., Weinstein, A.M. (eds.) Membrane Transport and Renal Physiology. The IMA Volumes in Mathematics and Its Applications, vol. 129, pp. 233–272. Springer, New York (2002)

Layton, A.T., Layton, H.E.: A semi-Lagrangian semi-implicit numerical method for models of the urine concentrating mechanism. SIAM J. Sci. Comput. **23**(5), 1526–1548 (2002)

Layton, A.T., Layton, H.E.: Countercurrent multiplication may not explain the axial osmolality gradient in the outer medulla of the rat kidney. Am. J. Physiol. Ren. Physiol. **301**, F1047–F1056 (2011)

Layton, A.T., Layton, H.E., Pannabecker, T.L., Dantzler, W.H.: The mammalian urine concentrating mechanism: hypotheses and uncertainties. Physiology **24**, 250–256 (2009)

Pannabecker, T.L., Dantzler, W.H., Layton, H.E., Layton, A.T.: Role of three-dimensional architecture in the urine concentrating mechanism of the rat renal inner medulla. Am. J. Physiol. Ren. Physiol. **295**, F1217–F1285 (2008)